Investigation of brain haemodynamics-metabolism relationship using mathematical modelling

End of Rotation 2 Report

London Interdisciplinary Biosciences Consortium
University College London

Student:

Miruna Serian

Supervisors:

Prof. Ilias Tachtsidis

Prof.Denis Mareschal

Abstract

Unraveling the complex relationship between brain haemodynamics and metabolism is important for our understanding of overall brain function, as well as for the understanding of various brain disorders. High brain activity is associated with high metabolic supply in a healthy brain, while mismatches between metabolism and neuronal activity might be observed in case of neuropsychiatric disorders or diseases. Mathematical modelling was used to simulate changes in the cytochrome-c-oxidase alongside haemodynamic changes in haemoglobin and deoxyheamoglobin during brain activation, measurements that would be obtained experimentally using broadband near-infrared spectroscopy (bNIRS). Different variations in systemic parameters were used to reflect different physiological brain states and to investigate the coupling between the brain haemodynamic and metabolic response to brain activation. The results suggest that a combination of mild decrease in arterial pressure, a more extreme decrease in partial pressure of CO_2 and different variations in a number of parameters reflecting the brain autoregulation state and mitochondrial health is responsible for most scenarios where mismatches between oxygen flow and metabolism were observed. It is hoped that mathematical modelling of the brain haemodynamic-metabolic response can be coupled with real experimental data to advance our understanding of brain physiology and cognitive functioning both in health and in disease.

Contents

Abbreviations and Acronyms

	Full Name
HHb	Haemoglobin
HbO_2	Deoxyhaemoglobin
CBF	Cerebral Blood Flow
oxCCO	oxidise Cytochrome C oxidase
fNIRS	Functional Near-Infrared Spectroscopy
bNIRS	Broadband Near-Infrared Spectroscopy
BOLD	Blood Oxygenation Level Dependent
CMRO2	Cerebral Metabolic Rate of Oxygen
BSX	BrainSignals Extended
SNS	Sympathetic Nervous System
eFAST	extended Fourier Amplitude Sensitivity Test
SI	First-order Sensitivity Index
ST	Total Sensitivity Index
fMRI	Functional magnetic resonance imaging
PET	Positron emission tomography

1 Introduction

The brain makes up only a small fraction of our total body mass, however, it represents the largest source of energy consumption, accounting for more than 20% of total oxygen metabolism. The high energy demand of the brain cells relative to most of the other tissues must be continuously satisfied by oxidative metabolism. Haemodynamic regulation maintains oxygen availability by adjusting the cerebral blood when variations in demand and supply happen [1]. Because different diseases and conditions can affect the normal functioning of these regulatory systems, the monitoring of brain oxygenation and metabolism have become of interest in clinical settings, with the development of neuroimaging techniques over the last decades allowing scientists to better understand the mechanisms underlying human brain function. One such technique is functional near-infrared spectroscopy (fNIRS), which is a portable and non-invasive technique allowing the monitoring of changes in the absorption spectra of naturally occurring chromophores [2].

fNIRS measures the changes in brain tissue concentration of oxygenated (HbO_2) and deoxygenated haemoglobin(HHb), which in turn, reflect the changes in cerebral blood flow (CBF) associated with neuronal activation, a phenomenon also known as neurovascular coupling [2]. fNIRS uses the absorption of light in the near infrared region of light (650–950nm), with the recorded changes in HHb and HbO_2 derived using the modified Beer-Lambert law. When neuronal activation happens, an increase in the metabolic demand for oxygen and glucose is observed. The increase in metabolic demands results in an oversupply of cerebral blood flow, which translates to an increase in the levels of HbO_2 and a decrease in HHb.

An extension to the fNIRS technique is broadband NIRS (bNIRS), which allows for the measurement of another chromophore, cytochrome-c-oxidase (CCO). Cytochrome-c-oxidase is the terminal electron acceptor in the electron transport chain and is responsible for more than 90% of ATP production, and can therefore, provide an indicator of cerebral cellular oxygen metabolism. bNIRS utilizes hundreds of NIR wavelengths, compared to the 2 or 3 wavelengths in the fNIRs range, and can quantify the redox state of cytochrome-c-oxidase (oxCCO) together with haemoglobin [3]. This form of measurement gained interest in the 1980s, however, measuring oxCCO accurately had proved to be challenging because of its low in-vivo concentrations [4], [5]. Changes in oxygenation levels are easier to measure, as HHb and HbO_2 are found in higher concentrations than oxCCO. However, it has been observed that oxCCO can provide more specific brain signals than haemoglobin [6], which might be explained by the fact that oxCCO is more concentrated in the intracerebral compartment and is less contaminated by extracerbral confounding. In contrast, haemoglobin signals can also be confounded by systemic contamination from extracerebral layers [7].

Recent developments in neuroimaging methods have allowed better and more accurate measurements of brain metabolic and activity signals using bNIRS [8], but it has not yet been widely adopted in clinical settings, partly due to difficulties in interpretation and the lack of commercially available instruments [9]. Several computational models of brain physiology have been developed to aid the understanding of bNIRS signals, with different approaches being taken, focusing on different functions, physiology or phenomena. The novel algorithms have helped overcome some of the challenges of the fNIRS and bNIRS techniques, allowing them to be successfully used in a number of clinical settings [10], [11].

Attempting to model the physiology of the brain and its complex behaviour is a challenging task. A number of models have been developed at UCL, all derived from the

models developed by Ursino and Lodi in 1997 [12] and 1998 [13]. One of the models is the BrainSignals model [14], which was designed to assist with the interpretation of haemoglobin levels and the oxidation state of cyctochrome-c-oxidase, derived from NIRS signals. The BrainSignals model is itself a simplification of a previous model, BrainCirc, which was developed a few years prior [15]. A further simplification of the BrainSignals model lead to the BrainSignals Extended (BSX) model, which allows the examination of confounding effects and extracerebral factors, such as blood pressure and oxygen saturation during NIRS experiments. These systemic changes can generate misleading results; for example, false negatives may hide any evidence of activation even though it was present and false positives may appear as activation when none occurred [16]. The BSX model can therefore, be a useful tool for investigating the haemodynamic response of the brain induced by variations in systemic factors and the underlying physiological state.

Model	**BrainCIRC**	**BrainSignals**	**BrainPiglet**	**BrainSignals Extended**	**BrainPigletHI**
Year	2005	2008	2013	2015	2015
Reactions	81	5	17	5	17
Differential equations	5	9	21	9	21
Algebraic relations	72	3	3	3	3
Variables	168	40	128	22	128
Parameters	697	139	226	73	227

Table 1: Table describing the BrainSignals family of models

In this report the BSX model was used to investigate the relationship between haemodynamics and metabolism using a method previously developed and used by Shokri-Kojori and colleagues, where they showed that alcohol intoxication could alter the relationship between neuronal activity and glucose metabolism [17]. The method was used more recently in a study by Pinti and colleagues (2021), which used the combined measurements of haemodynamic and metabolic activity (bNIRS), coupled with electrical (EEG) signals responses to show that in a healthy brain there typically is an agreement between energy supply and utilization [18]. As part of the analysis pipeline they developed, two indices describing the coupling between haemodynamics and metabolism are computed. The two indices - the relative power (rPWR) and relative cost (rCST)- can be used to generate two axes that reflect the magnitude and direction of the changes in HbO_2/HHb and oxCCO. By dividing the map into four quadrants, haemodynamic-metabolic responses can be grouped based on the extent to which the changes in HbO_2/HHb and oxCCO vary together or fall behind one another. It is expected that in a healthy functioning brain most of the responses would be situated in the upper right and lower left quadrants of the map (greater increase in HbO_2 and oxCCO, and greater decrease in HHb; greater decrease in HbO_2 and oxCCO and greater increase in HHb) while in an impaired or injured brain, the responses would be found in the upper left and lower right quadrants (greater increase in HbO_2 and decrease in oxCCO and HHb; greater decrease in HbO_2 and greater increase in HHb and oxCCO) (Fig. 1). The aim of this report was to use mathematical modeling to simulate brain activation in a healthy brain as well as simulate brain responses when different systemic parameters are varied. Further, the results were used to investigate the coupling between brain haemodynamics and metabolism. By simulating the brain using the BSX mathematical model, driven by variations in different systemic parameters to reflect different impaired brain states, potential physiological causes for mismatches between energy supply and utilization can be investigated. It is expected that certain combinations of parameters that are physiologically relevant could lead to

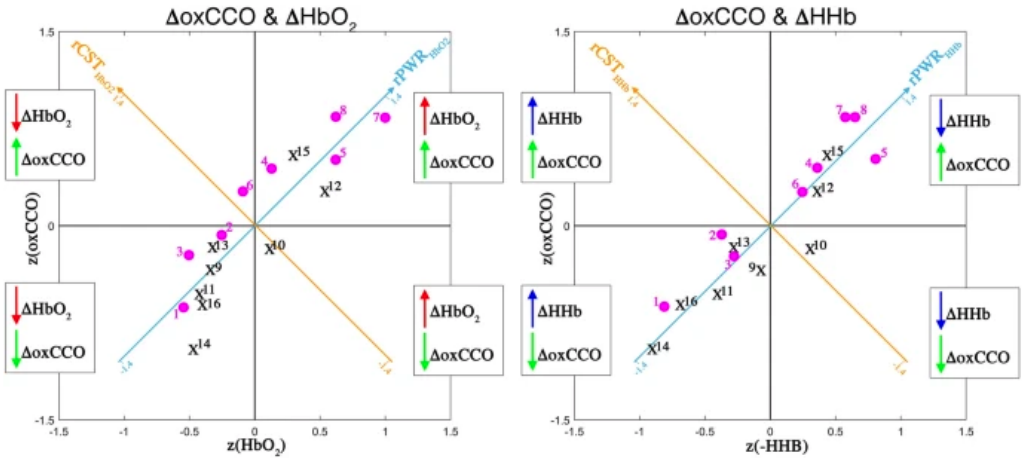

Figure 1: Visual representation of rPWR and rCST. In this study Pinti and colleagues looked at the haemodynamics and metabolism relationship during a passive visual stimulation in a healthy cohort. The plots show a significant mismatch between HHb and oxCCO for Channel 10, with changes in HHb exceeding the changes in oxCCO when compared to the rest of the channels. Figure adapted from [18]

a greater lag between activity demand and metabolic supply, which is common in case of neuropsychiatric disorders and disease.

2 Methods

2.1 Model structure

The BSX model is a mechanistic model that takes a bottom-up approach towards understanding brain's physiology [7]. The overall structure of the BSX model is depicted in Fig. 2. The model consists of two interacting departments - a haemodyanmic and a metabolic compartment, along with a scalp flow compartment. The haemodynamic compartment represents the blood flow and oxygen delivery to the brain tissue while the metabolic compartment describes oxygen consumption in the neuronal mitochondria. The scalp compartment is modelled as a separate compartment parallel to the brain haemodynamic compartment. Three systemic inputs, mean arterial pressure (Pa), arterial partial pressure of carbon dioxide ($PaCO_2$) and arterial oxygen saturation (SaO_2), along with metabolic demand (u), are the elements that drive the blood flow in the haemodynamic compartment.The metabolic demand is a control parameter which can be increased to indicate functional brain activation. The model reproduces the normal physiological response of maintaining blood flow through autoregulation, following pressure variation, vasoconstriction and vasodilation caused by changes in CO_2 and O_2. Various factors such as ambient temperature, blood CO_2 concentration as well as the sympathetic nervous systems have been known to influence scalp blood flow [19], [20]. The extracerebral blood flow compartment is directly affected by two

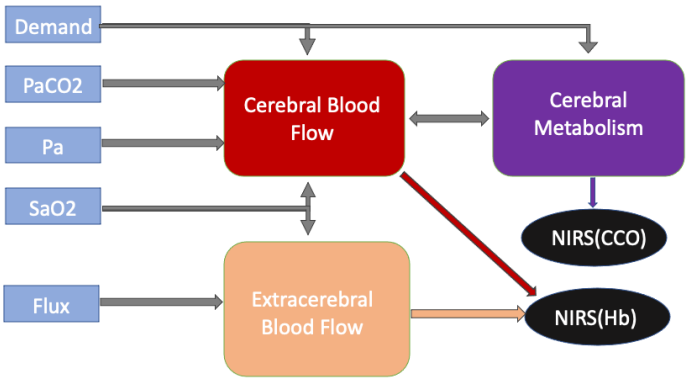

Figure 2: Main structure of the BSX model. Figure adapted from [7]

inputs - SaO_2 and $Flux$ - and is not directly influenced by neuronal activity, however, it can be affected by the SNS. Therefore, the blood scalp flow compartment depends on a subset of the same systemic variables as the cerebral compartment. However, its behaviour is not influenced by that of the cerebral blood flow. Apart from the the 5 'declared' input parameters (Pa, $PaCO_2$, SaO_2, u and $Flux$), the BSX model is also driven by a number of 72 independent parameters, and 49 derived parameters.

2.2 Software

The model was implemented in the open source Brain Circulation Model Developer (BCMD) environment, which uses the RADAU5 library [21] to numerically solve the models' differential-algebraic equation systems. The software and model implementations are available online. The BCMD environment installation required the gfortran package as well as an updated version of Python (in this report v3.8 was used) and Scipy [21]. More information about the installation requirements and steps can be found here. The BCMD environment comes with a GUI (Graphical User Interface) that can be used to run and plot individual simulations. However, due to the nature of the investigation in this report and the high number of simulations needed to run, the GUI was not a feasible option, and instead, several batch scripts written in Python were used to run and analyse the simulations. All the scripts written to run and analyse the simulations get be found here.

The course of a simulation is controlled by an input file with a simple yet not intuitive format, which specifies the simulation time steps and parameter changes as well as the options to reconfigure the the output. The input files are then used together with the compiled model to run batches of simulations. Examples of input files used to run the simulations can be found here.

All the simulations and analyses were run on a Quad-Core Intel Core i5 processor with a total number of 4 cores. A total number of 53,450 simulations were run in order to generate the results presented in this report.

2.3 Brain Simulations

Healthy data was simulated using the BSX model with the default parameter settings shown in Table 3. The healthy brain simulations were performed for different values of the demand parameter u to simulate brain activation. The demand parameter range considered for the healthy brain simulations is the default value $\pm 50\%$, which was decided to be physiologically relevant. In order to simulate an impaired brain during brain activation, the model was modified by changing either a single parameter or different combinations of parameters to reflect a potential pathology or injury. The demand parameter u was kept constant at a value of 1.5 for all the 'impaired' brain calculations to reflect brain activation. Parameters were decreased or increased from their default value by either 25% or 50%. For each of the brain scenarios that were not part of any of the sensitivity analyses, parameters were varied by equally sized increments, so that 50 simulations were run for each set of parameters or parameter combinations, covering the entire decided parameter range (i.e., 25 simulations for a 50% increase in u from its default value of 1 such that u is in range [1, 1.5] and 25 simulations for a 50% decrease in u from its default value of 1 such that u is in range [-0.5, 1]).

2.4 Data analysis

2.4.1 Integration of haemodynamic and metabolic data

The method used to analyse the relationship between metabolic and haemodynamic was developed by Shokri-Kojori [17] and further adapted to bNIRS data by Pinti and colleagues [18]. The method consists of performing a 45 of the haemodynamics-metabolism axes to compute two indices - rPWR and rCST. The relative power (rPWR) reflects the extent of concurrent changes in metabolism and haemodynamics, while the relative cost (rCST) indicates the extent to which energy supply exceeds or falls behind energy utilisation. High metabolic supply is associated with high neuronal activity in healthy brains, while a lag between activity demand and metabolic supply is common in case of neuropsychiatric disorders and diseases. High values of rPWR are usually observed in brain regions with a high metabolic demand while high levels of rCST are suggested to reflect the use of alternative metabolic pathways (e.g., aerobic glycolysis vs oxidative phosphorylation) or of alternative metabolic substrates (e.g., glucose vs ketone bodies)[17].

In this analysis the mean ΔHbO_2, ΔHHb and $\Delta oxCCO$ values for each simulation were calculated by z-scoring the signal changes in HbO_2, HHb and oxCCO (the difference between the signal at each time step and the signal at t=0) according to a baseline level, which was set as the 5 seconds prior to demand variation, followed by extraction of the mean responses during the brain activation window, which was set as a window of 10 seconds starting after a 5 seconds buffer following demand increase (in this report the activation window is between 125s and 135s). For each data set the rCST and rPWR values for both ΔHbO and ΔHHb were computed by performing a 45°rotation of the haemodynamics(oxCCO) and metabolism (HHb and HbO_2) axes. This generates a rPWR and rCST axis, where the rPWR axis corresponds to high metabolism+high demand (positive end) or low metabolism+low demand (negative end) and the rCST axis reflects high metabolism+low activity (positive end) or low metabolism+high demand (negative end). In a Cartesian system, the rPWR and rCST

values are computed as in the equation below:

$$\begin{bmatrix} rPWR \\ rCST \end{bmatrix} = \begin{bmatrix} cos(45°) & sin(45°) \\ -sin(45°) & cos(45°) \end{bmatrix} \begin{bmatrix} z(activity) \\ z(metabolism)) \end{bmatrix}$$

For each data set the z-scored mean ΔHbO_2 and ΔHHb values for each simulation of parameter/parameters change were plotted against the z-scored mean values of δoxCCO. The sign of the mean ΔHHb response was inverted so that the sign of $rPWR_{HHB}$ and $rCST_{HHb}$ matched that of $rPWR_{HbO_2}$ and $rCST_{HbO2}$. Dividing the plot into four equal quadrant made it possible to more easily visualise and understand the cases which exhibited a match or mismatch between metabolism and haemodynamics.

2.4.2 Sensitivity analysis

Sensitivity analysis is a powerful technique for understanding a model and its behaviour by analysing how the model's output is influenced by its inputs. The chosen sensitivity analysis method used in this report is the extended Fourier amplitude sensitivity test (eFAST) [22], [23], which was implemented using the SALib Python library [24]. The eFAST method estimates both a first-order sensitivity index (how much a parameter affects model output when varied alone) and a total sensitivity index (how influential the parameter is when interactions with all other parameters are considered). An Interaction Index was also computed by subtracting the first-order sensitivity index (SI) from the total sensitivity index (ST). Larger values of SI indicate a higher influence of the parameter on the output, while larger interaction index values indicate interactions with other parameters. A schematic of the modelling and analysis flow is found in Figure 3.

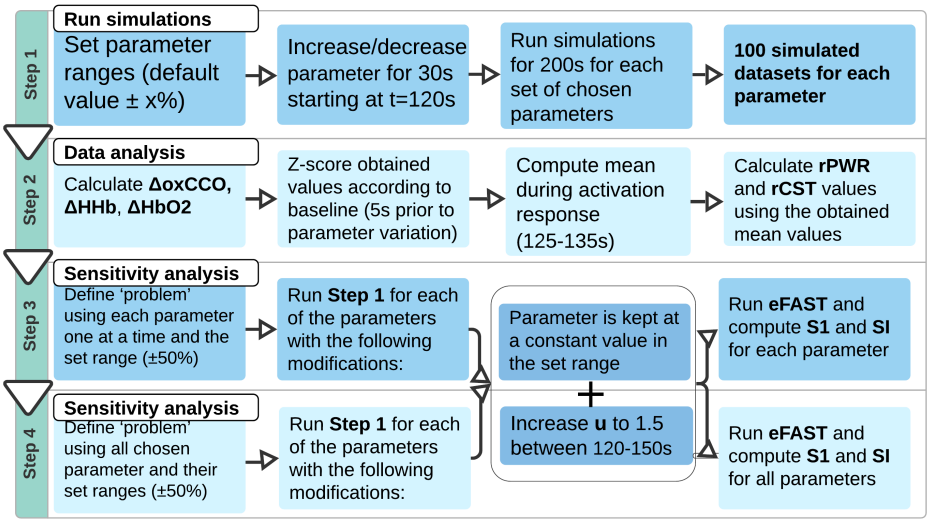

Figure 3: Model simulations and data analysis flow

3 Results

3.1 Brain response during activation

Functional brain activation increases the brain's metabolic demand for oxygen and glucose, leading to an oversupply of cerebral blood flow. As this process is mediated by several neurovascular mechanisms, an increase in CBF(Cerebral Blood Flow) produced an increase in HbO_2 and a decrease in HHb concentrations. This haemodynamic response is caused by a mismatch between the amount of oxygen that reaches the activated brain region (higher levels) and the rate at which it is consumed. The BSX model was used to simulate brain activation by increasing demand 50% from its default value and neuronal inhibition by decreasing demand 50% from its default value (Fig. 4). A 50% increase in demand caused an increase in ΔoxCCO concentration by around 0.15 μM and a decrease in the concentration of ΔHHb by around 1 μM. Haemoglobin levels showed an initial sharp increase by more than 2μM followed by a slow and short decrease in concentration as the increased conductance flow lead to a rise in tissue oxygen (Fig. 5c.). The levels of oxCCO showed a smaller increase of 0.10μM followed by a small decrease in concentration as the brain activation continued (Fig. 5f). On the other side, brain inhibition lead to a decrease in oxCCO concentration, proportional to the increase observed during brain activation. In the case of HHb, neuronal inhibition lead to an initial concentration increase of around 0.5 μM followed by a sharp decrease of 0.2 μM and then a slow decrease to a concentration of 0.25μM at the end of the inhibition. Haemoglobin (HbO_2) responded differently to inhibition with a smaller initial decrease and subsequent slow increase in concentration for the rest of the inhibition compared to the increase caused by brain activation.

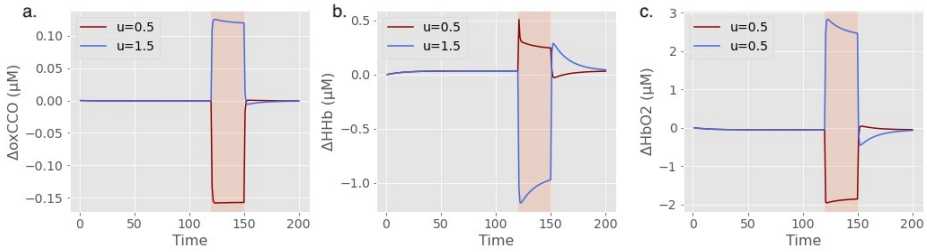

Figure 4: Neuronal activation and inhibition responses when the demand parameter u was increased to 1.5 (blue) and decreased to 0.5 (red) for oxCCO(a), HHb(b) and HbO_2(c). The orange coloured block represents the activation window when demand was varied from its default value.

To evaluate the relationship between brain haemodynamics and metabolism during brain activation and inhibition in a healthy brain, the rPWR and rCST parameters were calculated by combining the means in the 10s brain activation/inhibition window of ΔHbO_2 and ΔHHb with the mean response of ΔoxCCO. Figures 5 a. and b. show the haemodynamic and metabolic response plots when demand is varied from its default value by ±50%. The plots show a linear relationship between ΔHHb and ΔoxCCO (Fig 5 a.) and between ΔHbO_2 and ΔoxCCO (Fig. 5 b.) during activation (demand increase). Increasing the demand parameter leads to a greater increase in ΔHbO_2 and ΔoxCCO and a greater decrease in ΔHHb indicating a healthy brain response. However, neuronal inhibition appears to shift the haemodynamic-metabolic response

to the lower right quadrant of the plots, more pronounced in the case of HHb. At more extreme values of demand decrease (50% decrease) the relative cost values of both HHb and HbO shift towards more negative values, indicating that the decrease in HHb or increase in HbO_2 exceeds the decrease in oxCCO.

Since increasing demand by up to 50% is observed to cause concurrent changes in haemodynamic-metabolic response (high rPWR and low rCST), as expected in a normal healthy brain, a value of 1.5 for the demand parameter u was chosen for all the subsequent simulations and analyses to reflect brain activation.

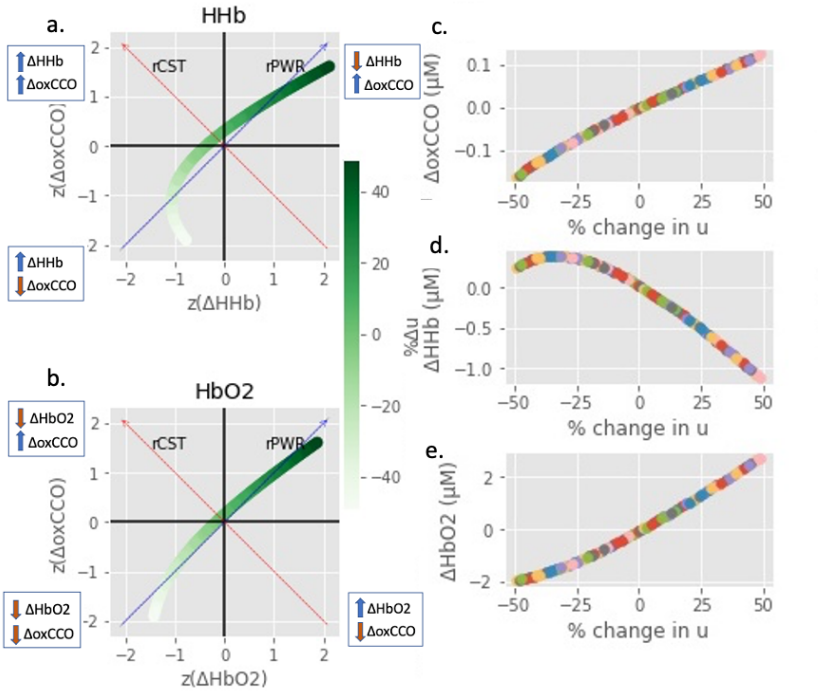

Figure 5: Neuronal activation and inhibition responses when the demand parameter u was varied by ±50% from its default value of 1 for oxCCO(c), HHb(d) and HbO_2(e). The y-axes represent the changes in concentrations from the baseline values, while the x-axes represent the percentage of variation in demand from the default value. Plots a. and b. describe the haemodynamic-metabolic response for HHb-oxCCO(a) and HbO_2-oxCCO(b). The y-axes represent the z-scored mean concentrations of oxCCO while the x-axes represent the z-scored mean concentrations of HHb or HbO_2. The responses are coloured according to the change in demand, with darker green corresponding to higher demand and white corresponding to low demand.

3.2 Sensitivity Analysis

In order to understand the contribution of the model parameters to the haemodynamic/metabolic response, sensitivity analysis was performed on an initial set of 31 parameters (the full list can be found in Table 3 in Supplementary data). When the parameters are varied individually while keeping the other parameters at their default

values, only a small number of parameters dominate the influence on the rPWR and rCST values. The top 11 parameters with the highest first-order sensitivity scores are shown in Fig. 6 and their full names and default values can be found in Table 2. Most of the parameters seem to affect the relative cost and power values of HHb and HbO_2 to a similar extent, with the exception of *phi*, which seems to have a greater influence on the rPWR and rCST of HHb than HbO_2. A number of the parameters identified, such as *R_auto*, *R_autu* and *k_aut* are dimensionless, which means that they have to be considered within the context of the model. *R_autu* and *R_auto* represent the autoreactivity to demand and oxygen, respectively, and an increase in any of them would mean an increase in the sensitivity of the autoregulatory response to either brain activation or oxygen concentration. *k_aut* is a parameter that describes the overall functioning of autoregulatory response, with lower values indicating an impaired autoregulatory mechanism. Other parameters include *P_V* and *r_n*, *phi*, *C_im*, *kCV*, *P_a* as well as the input parameters *P_a*, Pa_CO_2 and SaO_2sup.

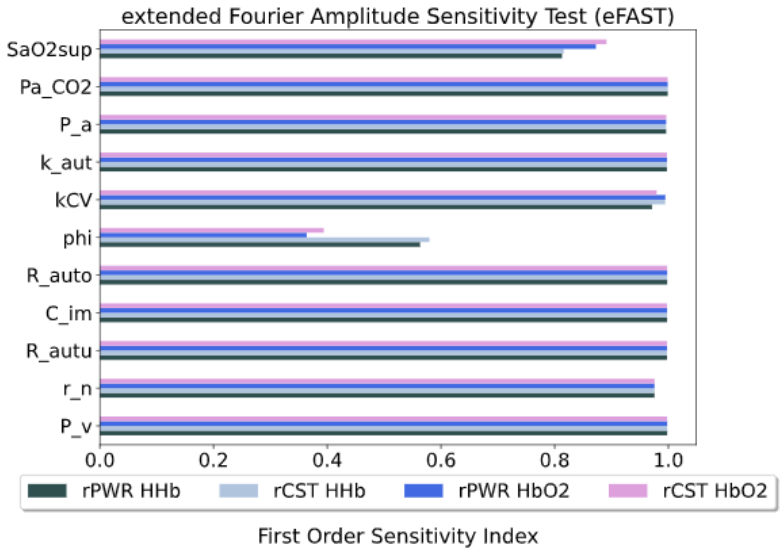

Figure 6: Top 11 parameters with the highest first-order sensitivity indices. The parameters were varied individually, one at a time and sensitivity indices were computed to assess their effect on the relative power and relative cost values of HHb/oxCCO and HbO_2/oxCCO.

Out of the 11 parameters with the highest sensitivity, only six of them were observed to shift the haemodynamics/metabolism response towards the upper left and lower right quadrants, indicating a mismatch between haemodynamics and metabolism and therefore, an 'impaired' brain (Fig. 7). Increasing *kCV* appears to initially cause a small increase in the rCST of both HHb and HbO_2, after which an increase in rPWR is observed and finally, the system seems to move towards negative values of rCST. Arterial pressure, P_a, maintains the levels of haemodynamics/metabolism in the top right and bottom left quadrants of the plot, indicating a match between haemodynamic and metabolic activity. However, at more extreme values, such as around 50% more or 50% less than the default value, the response shifts towards higher levels of rCST_{HHb} and rCST_{HbO_2}. Changes in *r_n* do not produce any fluctuations in the levels of $\Delta oxCCO$, however, increasing *r_n* leads to lower levels of both ΔHHb and ΔHbO_2, indicating a mismatch between haemodynamics and metabolic activity. While *phi* maintains the

Implementation name	Parameter	Default Value	Units
k_aut	Overall functioning of autoregulatory response	1	dimensionless
kCV	Factor relating the Complex V driving force to the membrane potential demand	0.02047339	mV^{-1}
P_a	Arterial blood pressure	100	$mmHg$
P_v	Venous blood pressure	4	$mmHg$
Pa_CO_2	Arterial partial pressure of carbon dioxide	40	$mmHg$
phi	Oxygen concentration at half-maximal saturation	0.036	mM
R_auto	Autoregulatory reactivity to oxygen	1.5	dimensionless
R_autp	Autoregulatory reactivity to blood pressure	1.54	dimensionless
R_autu	Autoregulatory reactivity to demand	0.5	dimensionless
r_n	Normal effective blood vessel radius	0.0187	cm
SaO_2sup	Arterial oxygen saturation	0.96	dimensionless

Table 2: Parameter names and definitions for the parameters with the highest sensitivities

response within the upper right and lower bottom quadrants when varied by 50% from its default value, it appears that at values exceeding this range the response shifts to an impaired state. Pa_CO_2 and P_v variations lead to high values of rCST of both HHb and HbO_2, with almost null rPWR values.

However, real biological systems are unlikely to operate in such constrained manner, and multiple parameter interactions are expected to cause physiological changes. While using the simplest modification of varying only one parameter at a time can still reflect real brain changes, the interactions of all the parameters or different combinations of parameters should be taken into account in order to better understand the behaviour of the system. For this reason, the parameters previously identified as having the highest sensitivities when varied individually were then varied jointly to asses their impact on the haemodynamics/metabolism response, as well as the interactions between them and the other parameters. As expected, all the parameters show a decrease in their effect on all the outputs when compared to their impact when varied one at the time. Most of the parameters have similar contributions for all of the considered outputs, with the exception of r_n, which has a greater effect on the relative cost and relative power values of HbO_2 than of HHb. In contrast, R_autu and P_v have more impact on the rCST and rPWR values of HHb than HbO_2. Interestingly, the c_im parameter appears to have no impact on the outputs when compared to the high sensitivity index of 1.0 observed when the parameter was changed individually and the rest of the parameters were kept at their default values. A similar behaviour is observed for SaO_2sup.

The interaction between the parameters becomes even more evident when considering their interaction index, which was calculated as the difference between the total sensitivity and the first-order sensitivity of each parameter. All the parameters show a higher interaction index than first-order sensitivity, underlining the interconnected and complex nature of the system. The interaction indexes of all the parameters are higher in the case of the rCST and rPWR values of HHb than those of HbO_2. Interestingly, both c_im and SaO_2sup appear to have little to no effect on the relative power and relative cost levels but seem to have a moderate level of interactions with the other parameters. The parameters with the highest overall first-order sensitivity index are Pa_CO_2, R_autu, r_n, P_a, P_v and k_aut. However, there is no clear relationship between the first-order identity indexes and the interaction indexes, with only P_v showing both a high effect on the outputs and a high level of interactions with the other parameters.

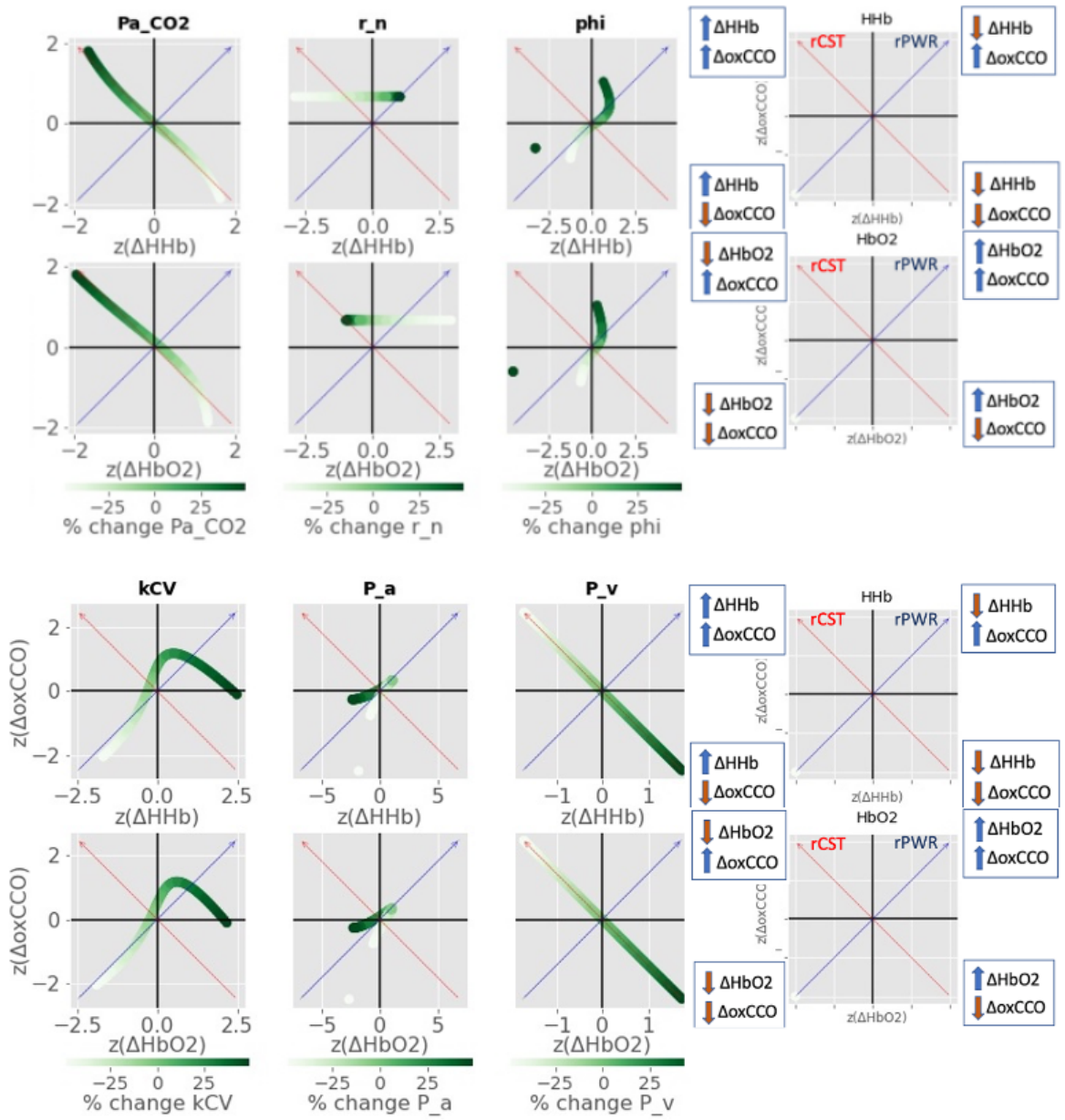

Figure 7: The haemodynamic-metabolic response during brain activation (u=1.5) when different systemic parameters were varied by ±50% from their default values. The y-axes represent the z-scored mean concentrations of oxCCO while the x-axes represent the z-scored mean concentrations of HHb or HbO_2. The responses are coloured according to the change in the specific parameter, with darker green corresponding to a higher parameter value and white corresponding to the lowest parameter value (decreased by 50%).

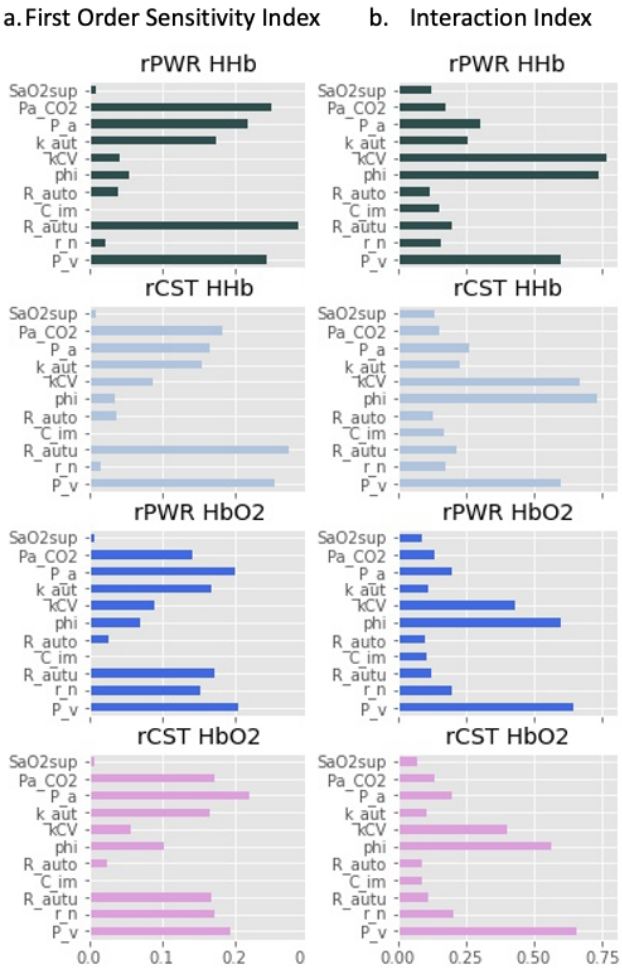

Figure 8: The first-order sensitivity index (a) and interaction index (b) of SaO_2sup, Pa_CO_2, P_a, k_aut, kCV, phi, R_auto, C_im, R_autu, r_n and P_v. The indexes were computed by running the model while varying all the parameters at the same time with different combinations of ranges. The interaction index was computed by subtracting the first-order sensitivity index from the total sensitivity index. Higher indexes corresponds to high sensitivities or higher interaction between the parameters.

3.3 Parameter interactions

A pathological or impaired brain state is usually the result of a combination of factors. In the context of mathematical modelling, the interaction between the systems parameters must be taken into account in order to understand its behaviour. The sensitivity analysis results identified a number of five parameters which have a large effect on the haemodynamic/metabolism response as well as a high level of interactions with the other parameters. The identified parameters are: phi, kCV, k_aut, P_a and Pa_CO_2. A series of brain activation simulations were further run using different combinations of the 5 parameters to reflect a pathology or injured brain state. The parameters were either decreased by 25% or 50% or decreased by 25% or 50% from their default value. This generated 1024 data sets as a result of a simple operation

of permuting with repetition (n=4, r=5). Taking a similar approach to the previous haemodynamics/metabolism analysis in this report, the rPWR and rCST values for each data set were computed along with the total number of simulations that resulted in a mismatch between haemodynamics and metabolism (equivalent to the top left and lower right quadrants in the rPWR/rCST plots). The different combinations of parameters were ordered according to the total number of 'impaired' situations and displayed as heatmaps.

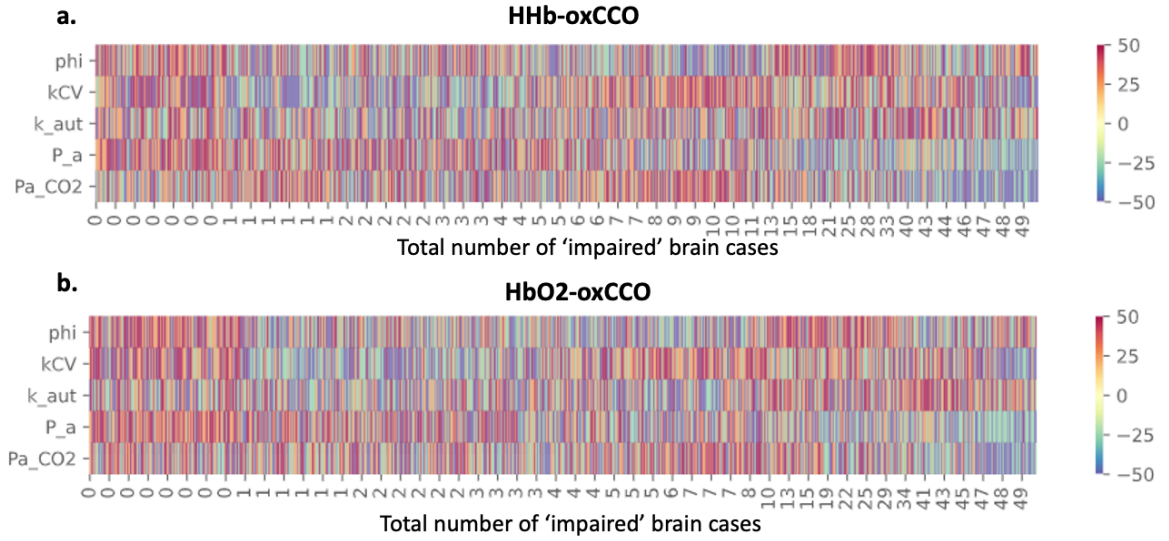

Figure 9: The combinations of different parameter variations and the number of 'impaired' brain scenarios observed for each set of combinations. The y-axes represent the parameters hat have the highest effect on the haemodynamic-metabolic response, and the x-axes represent the total number of 'impaired' brain states observed for each scenario. A brain response is considered 'impaired' if the response is found in the upper left or lower right quadrants when the z-scored ΔHHb/ΔHbO_2 values are plotted against the z-scored values of ΔoxCCO. Each combination of parameter range variations comprises of a data set of 50 simulations, therefore, a total number of 'impaired' brain states a combination can result in is 50. Cells coloured in dark blue correspond to a decrease of %50 in the respective parameter, while a lighter green represents a mild decrease of 25%. Similarly, cells coloured in red correspond to an increase of 50% in the respective parameter, while orange represents a mild increase of 25%.

Overall, the highest number of 'impaired' state responses were observed with a decrease in certain parameters such as kCV, P_a and Pa_CO_2 while most of the situations with no 'impaired' brain states appeared to result from a combinations of parameter increases. It was observed that for both HHb and HbO_2 cases the highest number of 'impaired' brain scenarios were caused, in general, by mild increases of only 25% in P_a and more extreme increases of 50% in Pa_CO_2, coupled with decreases in kCV by either 25% or 50%. k_aut increases of mostly 25% were also noted to be present in the cases with most 'impaired' brain scenarios in the haemodynamic-metabolic response of HbO_2.

4 Discussion

The results indicate that a small number of model parameters that are physiologically relevant such as P_a (arterial pressure), Pa_CO_2 (partial pressure of CO_2), phi (oxygen concentration at half saturation), kCV (factor relating the Complex V driving force to the membrane potential demand) and k_aut (factor describing the overall functioning of autoregulatory response) dominate the interaction between brain haemodynamics (HHb and HbO_2) and metabolism (oxCCO). The results could help investigate the possible causes and effects of physiological changes observed both in health and in disease.

Previous studies have demonstrated that high brain activity is associated with high metabolic supply in a healthy brain, while mismatches between metabolism and neuronal activity might be observed in case of neuropsychiatric disorders or diseases [17]. For example, Pinti and colleagues coupled bNIRS and EEG measurements with rPWR and rCST analysis to show that all cortical regions display a coordinated cerebral metabolism and haemodynamic activity. Only one case of significant mismatch between HHb and oxCCO was observed, which was suggested to be caused by the "blood stealing" phenomenon or a suppression of neuronal activity [18]. Previously, the same method coupled with fMRI and PET results (Positron Emission tomography) was used by Shokri-Kojori and colleagues to demonstrate how alcohol intoxication can alter the relationship between neuronal activity and glucose metabolism [17].

When a healthy brain area becomes active it is expected that the concentration of HbO_2 increases while that of HHb decreases. This is due to a phenomenon called neurovascular coupling, which follows neuronal activation, and causes an increase in the metabolic demand for oxygen and glucose. When a healthy brain was simulated by keeping all parameters at their default values and the demand was increased to 1.5 during the activation window, the concentration of deoxyhaemoglobin (ΔHHb dropped by around 1μM while that of haemoglobin (δHbO_2) increased by almost 3μM (Fig. 5b.). As expected, when integrating the measures of brain haemodynamics and metabolism extracted from the HbO_2, HHb and oxCCO data, increasing the demand parameter by up to 50% from its default value resulted in concurrent and greater increase in HbO_2 and oxCCO and greater decrease in HHb. In contrast, decreasing demand lead to an increase in deoxyhaemoglobin (HHb) and a decrease in haemoglobin (HbO_2) and oxCCO. The response is in accordance with previous studies which showed that decreases of HbO_2 and increases of HHb are associated with brain deactivation [25], with suppression of neuronal activities suggested to reduce the cerebral blood flow (CBF) which would result in an increase of HHb [26] [27]. When the demand was decreased between 25% and 50% from its default value of 1, higher values of rCST were observed, with a more pronounced effect on the HHb response. This suggests that neuronal inhibition can lead to a mismatch between oxygenation and metabolism, with changes in HHb and HbO_2 concentrations exceeding that of oxCCO. Although several visual stimulation studies in both animals [28] and humans [29] observed decreased BOLD (blood-oxygen-level-dependent) signals and decreased oxy-/increased deoxy-haemoglobin concentrations in the non-stimulated areas of the visual cortex as well as the areas corresponding to regions in the visual field not received the subjects attention [30], the relationship between the metabolic and haemodynamic response to neuronal inhibition is still not understood. Contrary to the results in this report, Stefanovic and colleagues found a consistent linear relationship between blood flow and oxygen consumption when using fMRI to investigate the changes in BOLD, cerebral blood flow and cerebral metabolic rate of oxygen consumption during neuronal

inhibition [31]. The shift in the response observed in this report might suggest that the demand parameter might not be physiologically accurate at more extreme levels (u¡0.75) or that the experiments used in the cited study did not cover a sufficiently high neuronal inhibition.

The relationship between brain haemodynamics and metabolism during activation becomes even more complex in situations where the brain is an impaired or injured state. Such situations were simulated by varying different systemic inputs at a time and generating a brain activation response by increasing the demand parameter u during the activation window. The top 11 parameters with the highest sensitivity scores have various physiological meanings including arterial blood pressure (P_a), venous blood pressure (P_v), arterial oxygen saturation (SaO_2sup), blood vessel radius (r_n) as well as the functioning of the autoregulatory response (k_aut, R_auto, R_autp, R_autu). All of these parameters showed similar effects across the relative power and relative costs of both HHb and HbO_2 with the exception of phi, which displayed higher sensitivity on the $rPWR_{HHb}$ and $rCST_{HHb}$ values than the $rPWR_{HbO_2}$ and $rCST_{HbO_2}$ values (Fig. 2. The haemodynamics-metabolism plots (Fig. 7) further revealed the extent to which the selected parameters affect the brain response. For example, variations of ±50% from the default values of venous pressure (P_v) and partial pressure of CO_2 ($PaCO_2$) lead to mismatches between both HHb/HbO_2 and oxCOO levels as indicated by the high positive levels of rCST when P_v was increased and Pa_CO_2 was decreased by 50%. In contrast, decreasing kCV, a factor relating the Complex V driving force to the membrane potential and demand appeared to cause a concurrent decrease in HbO_2 and oxCCO and increase in HHb, while increasing the parameter lead to higher values of $rPWR_{HbO_2}$ and $rCST_{HHb}$, especially at more extreme values. Another interesting case is that of variations in r_n, which do not cause any changes in oxCCO levels during brain activation but lead to variations in HHb and HbO_2 levels. Stiffening of blood vessels in the brain has been suggested as a potentially important factor in a number of pathologies such as Alzheimer's disease [32] as well as in autoregulation.

In practice, systemic factors are unlikely to vary in isolation, and variations of different combinations of parameters are responsible for different pathologies and diseases. The effect of the interactions of parameters with the highest individual sensitivities was outlined when the 11 parameters were varied together in different combinations (Fig. 8). Apart from SaO_2sup and C_im, which displayed almost null sensitivity on the haemodynamics-metabolism response outputs, all other parameters showed varying levels of sensitivities. Interestingly, only three of the parameters, kCV, phi and P_v appeared to have high interaction with the other parameters (around or above 0.5 Interaction Index value). When investigating the types of increase/decrease parameter value combinations that caused the higher number of 'impaired' brain scenarios (HHB/Hbo2-oxCCO responses situated in the upper left or lower right quadrants of the haemodynamics-metabolism plots), only a number of five parameters dominated the combinations space (Fig. 9). In the case of HHb, parameter variations in different combination of phi, kCV, k_aut, P_a and Pa_CO_2 were observed to affect the brain haemodynamics-metabolic response the most, while a clear pattern was harder to observe in the case of HbO_2. The results suggest that a decrease of 25% in P_a concentration coupled with a decrease of 50% in Pa_CO_2 concentration and with different combinations of parameter range increase/decreases in k_aut, kCV and phi concentrations account for the highest numbers of impaired brain states found in both HHb and HbO_2 responses. In the case of the HbO_2 haemodynamic-metabolic response, increases by either 25 or 50% in the k_aut concentration coupled with the decreases in P_a and Pa_CO_2 appeared to cause the highest cases of brain impairment.

It is not surprising that arterial pressure and partial pressure of CO_2 are responsible for mismatches between brain oxygenation and metabolism. Low blood pressure is typically accompanied by symptoms such as fatigue, dizziness and headaches and reduced cognitive performance, which is assumed to be the result of deficient regulation of cerebral blood flow [33]. In contrast to hypertension, which constitutes a significant risk factor for cardiovascular diseases, hypotension is not regarded as a severe condition. Nevertheless, hypotension can affect personal well-being and quality of life, having been associated with and increased degree of depressiveness [34] as well as higher incidence of Alzheimer's and vascular dementia [35]. It is possible that arterial pressure (P_a) and the partial pressure of CO_2 (Pa_CO_2) also play a role in speech tasks, with increase in arterial pressure being associated with fast speech as well as anxiety [36]. Therefore, possible mismatches between brain blood oxygenation and metabolism might be missed when speech tasks are used or the subject is anxious, as moderately high P_a and Pa_CO_2 levels were observed to be associated with the least number of 'impaired' brain responses. On the other side, mismatches in the metabolic-haemodynamic responses could also indicate underlying conditions such as Alzheimer's disease and dementia as well as chronic depression, which have been suggested to cause an altered cerebral metabolism coupled with lower cerebral blood flow reactivity [37]. Therefore, experimental results which show mismatches between brain haemodynamics and metabolism must be interpreted with caution.

The results also show that k_aut, an important factor describing the overall functioning of the autoregulatory response plays an important role in shifting the haemodynamic metabolic response towards an 'impaired' brain state. The functioning of the autoregulatory response is thus directly affecting the relationship between brain haemodynamics and metabolism. However, despite other parameters not directly controlling the autoregulation response, the interconectedness and complex nature of the brain model means that they could still control it indirectly. For example, the kCV parameter relates the Complex V driving force to the membrane potential and demand and might indirectly control blood flow during autoregulation, as inhibition of the mitochondrial membrane complexes could lead to reduced vascular dilation and further result in impaired cerebral vascular function [38]. Changes from its default value might indicate a mitochondrial complex V deficiency, which can affect the nervous system and the heart. Although most of the the symptoms accompanying certain conditions associated with mitochondrial complex V deficiency are present since birth, some symptoms accompanying certain conditions such a condition called neuropathy, ataxia, and retinitis pigmentosa (NARP) [39] and Leigh Syndrome [40] may appear later in life, for example in late childhood or early adulthood. Therefore, understanding the relationship between brain haemodynamics and metabolism might help elucidate the mechanisms causing the imbalance and might help early diagnosis of certain neurological conditions.

5 Conclusion

This report demonstrates the concurrent use of haemoglobin, deoxyhaemoglobin and cytochrome-c-oxidase signals to investigate the underlying causes and mechanisms of impaired haemodynamic and metabolic response during brain activation. By simulating different impaired or injured brain scenarios through the BSX brain model, it was observed that a number or parameters reflecting arterial blood pressure changes as well

as mitochondrial deficiencies play an important role in cases where altered metabolism and neurovascular coupling mechanisms were found. It is hoped that mathematical modelling of the brain haemodynamic-metabolic response can be coupled with real experimental data to advance our understanding of brain physiology and cognitive functioning both in health and in disease.

6 Future Work

In this report the Extended Brain Signals (BSX) model was used to simulate different brain scenarios. However, other brain physiology models such as the BrainPigletHI model developed at UCL [11] could be used to investigate the brain activation response in neonatal brains. Further, the effect of more extreme ranges of parameter changes could be investigated. Finally, real experimental data should be integrated with the simulation results for a better understanding of underlying mechanisms.

7 Limitations

The simulated scenarios are idealised and limited by the nature of the mathematical model, as some aspects of the BSX model are purposefully simplistic. For example, the scalp blood flow model does not take into account the influence of certain factors that might affect the skin blood flow such as the influence of the autonomic nervous system. Other factors such as heart rate, breathing rate and skin temperature could be introduced in the model to allow for improved behavioural simulation [7]. What is more, the lack of experimental data in this report means that real physiological conclusions are harder to extract from the simulation results only.

Another limiting factor in this report was the computational power necessary for running the number of simulations corresponding to the high number of combinations of various ranges and different parameter combinations to reflect certain brain pathologies. Exploring the increase/decrease of only 5 parameters by either 25% or 50% required more than 51 thousands simulations to be run which took a considerable amount of time. Performing the simulations on a GPU-connected system or a High Performance Computing (HPC) cluster could allow exploration of more complex brain scenarios.

8 Supplementary Data

Implementation name	Parameter	Default Value	Units
a	Concentration of oxidised cytochrome c oxidase	0.06567	mM
a_n	Normal concentration of oxidised cytochrome c oxidase	0.06567	mM
$bred$	Concentration of reduced cytochrome a3	0.001408	mM
$bred\_n$	Normal concentration of reduced cytochrome a3	0.001408	mM
c_im	Capacitance of the mitochondrial inner membrane	0.00675	$mMmV^{-1}$
$CMRO2\_n$	Normal metabolic rate of oxygen consumption	0.034	mMs^{-1}
$CMRO2$	Metabolic rate of oxygen consumption	0.034	mMs^{-1}
$cytox\_tot\_tis$	Concentration of cytochrome c oxidase in tissue	0.0055	mM
$dpsi$	Mitochondrial inner membrane potential	145	mV
$dpsi\_n$	Normal mitochondrial inner membrane potential	145	mV
H	Mitochondrial proton concentration	0.00003981	mM
H_n	Normal mitochondrial proton concentration	0.00003981	mM
k_aut	Overall functioning of autoregulatory response	1	dimensionless
$CBFn$	Normal cerebral blood flow	0.0125	$ml_{blood}ml_{blood}^{-1}s^{-1}$
kCV	Factor relating the Complex V driving force to the membrane potential demand	0.02047339	mV^{-1}
$O2\_n$	Normal mitochondrial oxygen concentration	0.024	$mmHg$
P_a	Arterial blood pressure	100	$mmHg$
P_an	Normal arterial blood pressure	100	$mmHg$
P_v	Venous blood pressure	4	$mmHg$
P_vn	Normal venous blood pressure	4	$mmHg$
Pa_CO_2	Arterial partial pressure of carbon dioxide	40	$mmHg$
phi	Oxygen concentration at half-maximal saturation	0.036	mM
R_auto	Autoregulatory reactivity to oxygen	1.5	dimensionless
R_autc	Autoregulatory reactivity to carbon dioxide	2.2	dimensionless
R_autp	Autoregulatory reactivity to blood pressure	1.54	dimensionless
R_autu	Autoregulatory reactivity to demand	0.5	dimensionless
r_n	Normal effective blood vessel radius	0.0187	cm
$SaO2\_n$	Arterial oxygen saturation	0.96	dimensionless
$Xtot$	Total concentration of haemoglobin O 2 binding sites in blood (4 times haemoglobin concentration)	9.1	mM
SaO_2sup	Arterial oxygen saturation	0.96	dimensionless

Table 3

References

[1] Ferenc Joó. "Cerebral Blood Flow and Metabolism by L. Edvinsson, E. T. MacKenzie, and J. McCulloch. Raven Press, New York, 1993, ISBN 0-88167-918-6". In: *Journal of Neurochemistry* 62.2 (2002), pp. 819–819. DOI: 10.1046/j.1471-4159.1994.62020819.x.

[2] Felix Scholkmann et al. "A review on continuous wave functional near-infrared spectroscopy and imaging instrumentation and methodology". In: *NeuroImage* 85 (2014), pp. 6–27. DOI: 10.1016/j.neuroimage.2013.05.004.

[3] Subhabrata Mitra et al. "Cerebral Near Infrared Spectroscopy Monitoring in Term Infants With Hypoxic Ischemic Encephalopathy—A Systematic Review". In: *Frontiers in Neurology* 11 (2020). DOI: 10.3389/fneur.2020.00393.

[4] A. D. Edwards et al. "Quantification of concentration changes in neonatal human cerebral oxidized cytochrome oxidase". In: *Journal of Applied Physiology* 71.5 (1991), pp. 1907–1913. DOI: 10.1152/jappl.1991.71.5.1907.

[5] F. Jobsis. "Noninvasive, infrared monitoring of cerebral and myocardial oxygen sufficiency and circulatory parameters". In: *Science* 198.4323 (1977), pp. 1264–1267. DOI: 10.1126/science.929199.

[6] Christina Kolyva et al. "Cytochrome c oxidase response to changes in cerebral oxygen delivery in the adult brain shows higher brain-specificity than haemoglobin". In: *NeuroImage* 85 (2014), pp. 234–244. DOI: 10.1016/j.neuroimage.2013.05.070.

[7] Matthew Caldwell et al. "Modelling confounding effects from extracerebral contamination and systemic factors on functional near-infrared spectroscopy". In: *NeuroImage* 143 (2016), pp. 91–105. DOI: 10.1016/j.neuroimage.2016.08.058.

[8] Gemma Bale et al. "A new broadband near-infrared spectroscopy system for in-vivo measurements of cerebral cytochrome-c-oxidase changes in neonatal brain injury". In: *Biomedical Optics Express* 5.10 (2014), p. 3450. DOI: 10.1364/boe.5.003450.

[9] Hellmuth Obrig. "NIRS in clinical neurology — a 'promising' tool?" In: *NeuroImage* 85 (2014), pp. 535–546. DOI: 10.1016/j.neuroimage.2013.03.045.

[10] Pardis Kaynezhad et al. "Quantification of the severity of hypoxic-ischemic brain injury in a neonatal preclinical model using measurements of cytochrome-c-oxidase from a miniature broadband-near-infrared spectroscopy system". In: *Neurophotonics* 6.04 (2019), p. 1. DOI: 10.1117/1.nph.6.4.045009.

[11] Matthew Caldwell et al. "Modelling Blood Flow and Metabolism in the Preclinical Neonatal Brain during and Following Hypoxic-Ischaemia". In: *Plos One* 10.10 (2015). DOI: 10.1371/journal.pone.0140171.

[12] M. Ursino et al. "Intracranial pressure dynamics in patients with acute brain damage". In: *Journal of Applied Physiology* 82.4 (1997), pp. 1270–1282. DOI: 10.1152/jappl.1997.82.4.1270.

[13] Mauro Ursino, Marco Giulioni, and Carlo Alberto Lodi. "Relationships among cerebral perfusion pressure, autoregulation, and transcranial Doppler waveform: a modeling study". In: *Journal of Neurosurgery* 89.2 (1998), pp. 255–266. DOI: 10.3171/jns.1998.89.2.0255.

[14] Murad Banaji et al. "A Model of Brain Circulation and Metabolism: NIRS Signal Changes during Physiological Challenges". In: *PLoS Computational Biology* 4.11 (2008). DOI: 10.1371/journal.pcbi.1000212.

[15] Murad Banaji et al. “A physiological model of cerebral blood flow control”. In: *Mathematical Biosciences* 194.2 (2005), pp. 125–173. DOI: 10.1016/j.mbs.2004.10.005.

[16] Ilias Tachtsidis and Felix Scholkmann. “False positives and false negatives in functional near-infrared spectroscopy: issues, challenges, and the way forward”. In: *Neurophotonics* 3.3 (2016), p. 030401. DOI: 10.1117/1.nph.3.3.030401.

[17] Ehsan Shokri-Kojori et al. “Correspondence between cerebral glucose metabolism and BOLD reveals relative power and cost in human brain”. In: *Nature Communications* 10.1 (2019). DOI: 10.1038/s41467-019-08546-x.

[18] P. Pinti et al. “An analysis framework for the integration of broadband NIRS and EEG to assess neurovascular and neurometabolic coupling”. In: *Scientific Reports* 11.1 (2021). DOI: 10.1038/s41598-021-83420-9.

[19] P.m. Netten et al. “Evaluation of Two Sympathetic Cutaneous Vasomotor Reflexes Using Laser Doppler Fluxmetry”. In: *International Journal of Microcirculation* 16.3 (1996), pp. 124–128. DOI: 10.1159/000179161.

[20] Hideaki Kashima, Tsukasa Ikemura, and Naoyuki Hayashi. “Regional differences in facial skin blood flow responses to the cold pressor and static handgrip tests”. In: *European Journal of Applied Physiology* 113.4 (2012), pp. 1035–1041. DOI: 10.1007/s00421-012-2522-6.

[21] Ernst Hairer and Gerhard Wanner. “Solving Ordinary Differential Equations II”. In: *Springer Series in Computational Mathematics* (1996). DOI: 10.1007/978-3-642-05221-7.

[22] A. Saltelli, S. Tarantola, and K. P.-S. Chan. "A Quantitative Model-Independent Method for Global Sensitivity Analysis of Model Output". In: *Technometrics* 41.1 (1999), pp. 39–56. DOI: 10.1080/00401706.1999.10485594.

[23] R. I. Cukier et al. "Study of the sensitivity of coupled reaction systems to uncertainties in rate coefficients. I Theory". In: *The Journal of Chemical Physics* 59.8 (1973), pp. 3873–3878. DOI: 10.1063/1.1680571.

[24] Jon Herman and Will Usher. "SALib: An open-source Python library for Sensitivity Analysis". In: *The Journal of Open Source Software* 2.9 (2017), p. 97. DOI: 10.21105/joss.00097.

[25] Kaoru Sakatani et al. "Changes of cerebral blood oxygenation and optical pathlength during activation and deactivation in the prefrontal cortex measured by time-resolved near infrared spectroscopy". In: *Life Sciences* 78.23 (2006), pp. 2734–2741. DOI: 10.1016/j.lfs.2005.10.045.

[26] P. T. Fox and M. E. Raichle. "Focal physiological uncoupling of cerebral blood flow and oxidative metabolism during somatosensory stimulation in human subjects." In: *Proceedings of the National Academy of Sciences* 83.4 (1986), pp. 1140–1144. DOI: 10.1073/pnas.83.4.1140.

[27] K.J. Mullinger et al. "Evidence that the negative BOLD response is neuronal in origin: A simultaneous EEG–BOLD–CBF study in humans". In: *NeuroImage* 94 (2014), pp. 263–274. DOI: 10.1016/j.neuroimage.2014.02.029.

[28] A. Shmuel et al. "Decreases in neuronal activity and negative BOLD response in non-stimulated regions of monkey V1". In: *Journal of Vision* 4.8 (2004), pp. 16–16. DOI: 10.1167/4.8.16.

[29] Andrew T. Smith, Adrian L. Williams, and Krishna D. Singh. "Negative BOLD in the visual cortex: Evidence against blood stealing". In: *Human Brain Mapping* 21.4 (2004), pp. 213–220. DOI: 10.1002/hbm.20017.

[30] Roger B.H Tootell et al. "The Retinotopy of Visual Spatial Attention". In: *Neuron* 21.6 (1998), pp. 1409–1422. DOI: 10.1016/s0896-6273(00)80659-5.

[31] Bojana Stefanovic, Jan M Warnking, and G.Bruce Pike. "Hemodynamic and metabolic responses to neuronal inhibition". In: *NeuroImage* 22.2 (2004), pp. 771–778. DOI: 10.1016/j.neuroimage.2004.01.036.

[32] Timothy M Hughes, Suzanne Craft, and Oscar L Lopez. "Review of 'the potential role of arterial stiffness in the pathogenesis of Alzheimer's disease'". In: *Neurodegenerative Disease Management* 5.2 (2015), pp. 121–135. DOI: 10.2217/nmt.14.53.

[33] Stefan Duschek and Rainer Schandry. "Reduced brain perfusion and cognitive performance due to constitutional hypotension". In: *Clinical Autonomic Research* 17.2 (2006), pp. 69–76. DOI: 10.1007/s10286-006-0379-7.

[34] E Barrett-Connor and L A Palinkas. "Low blood pressure and depression in older men: a population based study". In: *BMJ* 308.6926 (1994), pp. 446–149. DOI: 10.1136/bmj.308.6926.446.

[35] G. Zuccala et al. "Hypotension and cognitive impairment: Selective association in patients with heart failure". In: *Neurology* 57.11 (2001), pp. 1986–1992. DOI: 10.1212/wnl.57.11.1986.

[36] Wolf Ursula, Wolf Martin, and Scholkmann Felix. "Even Arts speech therapy with inner speech affects arterial partial CO2 pressure, cerebral haemodynamics

and oxygenation–a functional NIRS study". In: *European Journal of Integrative Medicine* 4 (2012), pp. 104–105. DOI: 10.1016/j.eujim.2012.07.717.

[37] H Tiemeier. "Cerebral haemodynamics and depression in the elderly". In: *Journal of Neurology, Neurosurgery Psychiatry* 73.1 (2002), pp. 34–39. DOI: 10.1136/jnnp.73.1.34.

[38] David W. Busija and Prasad V. Katakam. "Mitochondrial Mechanisms in Cerebral Vascular Control: Shared Signaling Pathways with Preconditioning". In: *Journal of Vascular Research* 51.3 (2014), pp. 175–189. DOI: 10.1159/000360765.

[39] Mark Rawle and Andrew Larner. "NARP Syndrome: A 20-YearFollow-Up". In: *Case Reports in Neurology* 5.3 (2013), pp. 204–207. DOI: 10.1159/000357518.

[40] Emma Ciafaloni et al. "Maternally inherited Leigh syndrome". In: *The Journal of Pediatrics* 122.3 (1993), pp. 419–422. DOI: 10.1016/s0022-3476(05)83431-6.